A SUB-12 GHZ UWB-TO-NARROWBAND RECONFIGURABLE ANTENNA USING VARACTOR DIODES SCALABLE FOR 6G IRS METASURFACES

Chai Han Ming[1], Shaharil Mohd Shah[2], Huda A Majid[3], Zuhairiah Zainal Abidin[4], Saizalmursidi Md Mustam[5], Nor Surayahani Suriani[6], Munirah Az Zahra Abdul Rashid[7]

ABSTRACT

This work presents a UWB-to-narrowband reconfigurable microstrip patch antenna using varactor diodes, developed as a tunable unit cell architecture intended for intelligent reflecting surfaces (IRS) in future 6G communication systems. While evaluated at sub-12 GHz frequencies for prototype verification, the proposed design methodology is inherently scalable to millimetre-wave bands. The proposed antenna initially exhibits an ultra-wideband (UWB) response from 3.22 GHz to 11.26 GHz, covering an 8.04 GHz bandwidth. By integrating two SMV1405-040LF varactor diodes, the antenna's operational mode is dynamically reconfigured to a narrower band from 5.11 GHz to 5.83 GHz (0.72 GHz bandwidth), targeting WLAN frequencies. The design inherits its geometry from a slotted UWB configuration to ensure structural stability and enable direct performance comparisons across tuning implementations. A reference configuration using copper bridges replaces the varactor diodes to emulate ideal switching conditions, thereby isolating the effects of active tuning. Results confirm that bandwidth reconfigurability is achieved with minimal impact on gain and efficiency. The antenna demonstrates effective radiation control and tuning behavior, confirming its suitability for frequency-agile IRS metasurfaces. This approach offers a practical pathway for signal propagation optimization in 6G wireless networks operating in the Ka-band.

Keywords: UWB-to-Narrowband, Reconfigurable antenna, Varactor diodes, 6G IRS applications, Ka-band

[1] Graduate Researcher, Department of Electronic Engineering, Universiti Tun Hussein Onn Malaysia (UTHM), 86400 Parit Raja, Johor, Malaysia, +60-7-4537000, Email: isaginji@gmail.com
[2] Associate Professor, Department of Electronic Engineering, Universiti Tun Hussein Onn Malaysia (UTHM), 86400 Parit Raja, Johor, Malaysia, +60-7-4537000, Email: shaharil@uthm.edu.my
[3] Associate Professor, Department of Electrical Engineering Technology, Universiti Tun Hussein Onn Malaysia (UTHM), 86400 Parit Raja, Johor, Malaysia, +60-7-4537000, Email: mhuda@uthm.edu.my
[4] Associate Professor, Department of Electronic Engineering, Universiti Tun Hussein Onn Malaysia (UTHM), 86400 Parit Raja, Johor, Malaysia, +60-7-4537000, Email: zuhairia@uthm.edu.my
[5] Senior Lecturer, Department of Electronic Engineering, Universiti Tun Hussein Onn Malaysia (UTHM), 86400 Parit Raja, Johor, Malaysia, +60-7-4537000, Email: saizal@uthm.edu.my
[6] Associate Professor, Department of Electronic Engineering, Universiti Tun Hussein Onn Malaysia (UTHM), 86400 Parit Raja, Johor, Malaysia, +60-7-4537000, Email: nsuraya@uthm.edu.my
[7] Application Engineer, R&D Applications, Avery Dennison Smartrac, 09000 Kulim, Kedah, Malaysia, +60-4-4019100, Email: azzahramunirah@gmail.com

Manuscript received on 08 April 2026, revised on 9 July 2026 and accepted on 10 July 2026 as per publication policies of *NED University Journal of Research*.

https://doi.org/10.35453/NEDJR-Icon3E2025-002-R1

1. INTRODUCTION

The rapid advancement of wireless communication technology has ushered in the development of the sixth-generation (6G) networks, which aim to deliver ultra-high data rates, low latency, and massive device connectivity. In order to meet these demands, the Ka-band (26.5–40 GHz) has been identified as a promising frequency spectrum for high-capacity communication due to its wide bandwidth and low interference potential [1], [2]. However, signal propagation at these high frequencies suffers significantly from path loss and penetration limitations. In order to address these challenges, Intelligent Reflecting Surfaces (IRSs) which comprise of passive or semi-passive metasurfaces with tunable electromagnetic (EM) responses have emerged as a viable solution for smart signal control and coverage extension [3], [4]. A key component of IRS systems is the unit cell, which must be capable of dynamically adapting its reflection characteristics across a range of frequencies. Traditionally, fixed-band metasurfaces have limited adaptability in practical environments. Hence, recent studies have explored the integration of tunable components such as PIN diodes, MEMS, and varactor diodes to enable dynamic reconfigurability [5], [6]. Among these, varactor diodes offer continuous tuning and relatively low power consumption, making them attractive for high-frequency reconfigurable antennas and metasurfaces [7].

Numerous designs have been proposed to achieve bandwidth and frequency reconfigurability using varactor-based techniques. For instance, a reconfigurable antenna in [8] used varactors to switch between Wi-Fi and WiMAX bands, while [9] demonstrated continuous wideband tuning using MEMS capacitors integrated on a microstrip patch. However, most of these efforts are limited to narrow frequency tuning or low-frequency operation (e.g., below 10 GHz), and very few focus on adaptable antennas that can transition between ultra-wideband (UWB) and narrowband modes. The critical research gap addressed in this study is the lack of single-element architectures capable of dynamically transforming their fundamental operational mode from a passive wide-spectrum sensor to a high-selectivity narrowband radiator. This work addresses this gap by implementing an integrated slot-and-varactor architecture that achieves a structural mode transformation while maintaining polarization and structural stability, serving as an foundational layout for high-frequency agile unit cells. Furthermore, while the use of IRSs in the Ka-band is still under investigation, the foundational elements such as frequency-agile antennas remain underexplored, especially those that can scale into IRS unit cells. In addition, many studies do not adequately benchmark the performance of tuned versus non-tuned structures to validate the effectiveness of their reconfiguration mechanisms. While the current study demonstrates proof-of-concept operation around 5 GHz for ease of prototyping and validation, the design architecture is inherently scalable to Ka-band (26.5–40 GHz). By proportionally reducing the physical dimensions of the radiating structure and employing high-frequency tuning components, the proposed antenna can be adapted for Ka-band IRS unit cells. This scalability path has been considered in the design evolution to ensure relevance for future 6G implementations.

Building on these limitations and scalability considerations, it is important to highlight recent advances in reconfigurable antennas and IRS-enabled architectures that provide further context for the present work. For instance, a metamaterial-inspired, varactor-tuned antenna enabling both frequency reconfigurability and pattern diversity was demonstrated in [10], while a Ka-band beam-scanning leaky-wave antenna using reconfigurable spoof surface plasmon polaritons has also been realized, illustrating dynamic beam control in the 25–30 GHz range [11]. Similarly, a 32×32 unit-cell reflectarray metasurface prototype achieved 20–25 dB signal enhancement across 5G mm-wave bands [12], confirming the utility of metasurfaces for practical coverage enhancement. Other approaches include epsilon-negative transmission-line antennas that enable compact frequency reconfigurability [13], varactor-based dual-polarized mm-wave arrays for mobile applications [14], and large-scale RIS designs employing over a thousand tunable elements for beam steering at mm-waves [15]. In addition, fully-addressable varactor-based metasurfaces supporting dual-linear polarization have been demonstrated [16], while RF MEMS-based reconfigurable patch antennas continue to provide efficient multiband operation [17]. Expanding beyond conventional multiband systems, a dual-mode switching architecture enabling explicit wide-to-narrowband state transitions has also been explored for cognitive radio networks [18]. Collectively, these studies reinforce the motivation and relevance of the present work, which focuses on UWB-to-narrowband reconfigurability as a scalable approach toward Ka-band IRS unit cells for future 6G applications.

In this paper, a tunable microstrip patch antenna is proposed, capable of transitioning between ultra-wideband (UWB) and narrowband operation through the integration of SMV1405-040LF varactor diodes. The antenna is fabricated on a low-cost FR-4 substrate, featuring a relative dielectric constant, εr of 4.3, a loss tangent, tan δ of 0.019, and a thickness, h of 1.6 mm. Designed and simulated using CST Microwave Studio®, the antenna operates over a broad frequency range of 3.22–11.26 GHz in its default configuration and can be reconfigured to a narrower band of 5.11–5.83 GHz via voltage-controlled capacitance. While this work demonstrates operation at sub-Ka-band frequencies, it proposes a design architecture that is scalable to Ka-band IRS implementations, serving as a foundation for future integration into intelligent reflecting surfaces (IRS) in 6G communication systems.

2. ANTENNA DESIGN AND SIMULATION

The antenna design evolved through several stages, beginning with a basic UWB configuration and culminating in a fully reconfigurable structure suitable for IRS unit cell applications. Optimization was performed by modifying both the microstrip patch and ground plane geometries, with simulations carried out using CST Microwave Studio® to progressively align the antenna response with the target frequency range. Four antenna configurations were developed as follows:

(a) Antenna 1 – Baseline UWB Antenna
(b) Antenna 2 – Enhanced UWB Antenna with Slotted Ground Plane
(c) Antenna 3 – Reconfigurable UWB-to-Narrowband Antenna using Varactor Diodes
(d) Antenna 4 – Reference Model with Copper Bridges for Ideal Switching Simulation

This modular design evolution supports future adaptation into IRS unit cells, where controlled bandwidth and radiation characteristics are critical for intelligent beam manipulation. Antennas 3 and 4 retain the same geometry and dimensions as Antenna 2, ensuring that any performance differences are solely due to the tuning mechanism. This design consistency enables an isolated evaluation of varactor-based reconfigurability versus ideal switching behavior. **Figure 1** illustrates the progressive evolution of the proposed antenna design. In **Figure 1**(a), the Baseline UWB Antenna (Antenna 1) serves as the foundational structure. In order to enhance impedance bandwidth, two rectangular slots are introduced in the ground plane, resulting in the Enhanced UWB Antenna with Slotted Ground Plane (Antenna 2) shown in **Figure 1**(b). Building on this configuration, **Figure 1**(c) presents the Reconfigurable UWB-to-Narrowband Antenna Using Varactor Diodes (Antenna 3), which integrates two SMV1405-040LF varactor diodes on the radiating patch to enable voltage-controlled bandwidth tuning. Finally, **Figure 1**(d) shows the Reference Model with Copper Bridges for Ideal Switching Simulation (Antenna 4), which mimics ideal switching by replacing the varactors with conductive bridges, allowing direct comparison of reconfigurable versus passive implementations.

The baseline UWB antenna (Antenna 1) is designed using a microstrip-line feeding technique, offering simplicity in fabrication and ease of integration with planar circuits. The radiating element consists of a hybrid geometry that combines a semi-circular patch with a rectangular extension. This geometry is chosen to excite multiple resonant modes and achieve a wide operational bandwidth, as it effectively supports smooth impedance transitions over a broad frequency range. The antenna is fabricated on an FR-4 epoxy substrate with a relative dielectric constant (εr) of 4.3, a loss tangent (tan δ) of 0.019, and a thickness (h) of 1.6 mm. The chosen substrate provides a cost-effective platform for prototyping at sub-6 GHz frequencies, although it introduces moderate dielectric losses at higher frequencies. It is acknowledged that FR-4 is unsuitable for Ka-band applications due to its high loss tangent (tan δ = 0.019), which introduces catastrophic dielectric losses at millimetre-wave frequencies and severely degrades total radiation efficiency. In this study, FR-4 is chosen strictly as a cost-effective, easily machinable platform for baseline proof-of-concept validation at microwave frequencies (sub-12 GHz). In order to transition this architecture to true Ka-band (26.5 – 40 GHz) IRS operations, a dual-step scalability pathway must be executed: first, a geometric reduction by a scaling factor, $S \approx 6$ must be applied to all physical features (L_{sub}, W_{sub}, R), and second, the substrate must be replaced with ultra-low-loss materials such as Rogers RT/Duroid 5880 (tan δ ≈ 0.0009) or Taconic TLY. The present work therefore uses FR-4 to demonstrate the concept at lower frequency while providing a roadmap for transition to more suitable materials in high-frequency operation. The total substrate size is 24 mm × 32 mm, optimized to balance performance and compactness.

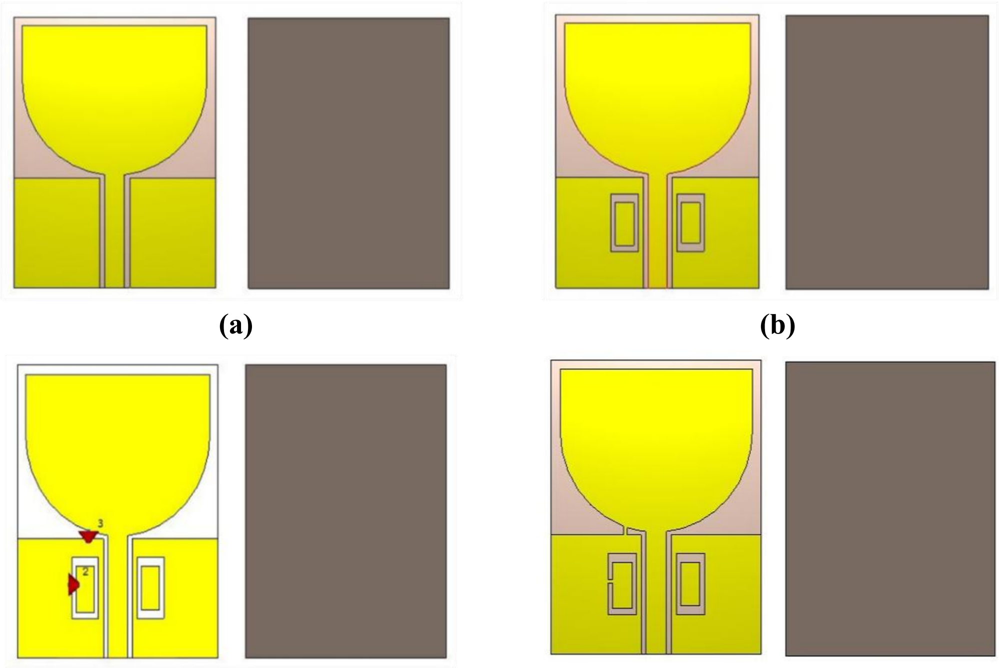

(a) **(b)**

(c) **(d)**

Figure 1. Evolution of the antenna design: (a) Antenna 1 - Baseline UWB Antenna; (b) Antenna 2 - Enhanced UWB Antenna with Slotted Ground Plane; (c) Antenna 3 - Reconfigurable UWB-to Narrowband Antenna using Varactor Diodes; (d) Antenna 4 - Reference Model with Copper Bridges for Ideal Switching Simulation

The microstrip feed line, along with the radiating patch, is made from copper with a standard thickness of 0.035 mm. A partial ground plane is employed on the reverse side of the substrate. Unlike conventional full-ground configurations, the partial ground plane enhances bandwidth by reducing the image current cancellation and enabling stronger coupling between the feed line and the patch. **Figure 2** shows the top and side views of the antenna geometry.

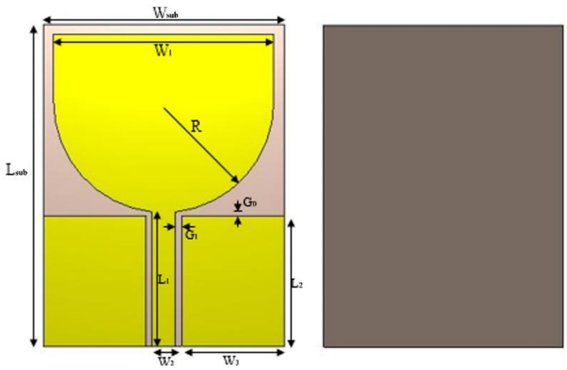

(a) **(b)**

Figure 2. Dimensions of Antenna 1 – Baseline UWB Antenna: (a) Top view; (b) Bottom view

As illustrated in **Figure 2**(a), the ground plane is located asymmetrically on either side of the feed line, leaving a significant open region that allows for additional tuning or matching enhancements in subsequent design iterations. This baseline configuration forms the foundation for further performance enhancements and tunability introduced in later design stages. **Table 1** details the critical design parameters.

Table 1. Dimensions (in mm) of Antenna 1

Parameters	Dimensions (mm)	Parameters	Dimensions (mm)
L_{sub}	32	W_2	2.3
W_{sub}	24	W_3	10.3
L_1	13.36	R	11
L_2	13	G_0	0.3
W_1	22	G_1	0.55

2.1 Antenna 2 – Enhanced UWB Antenna with Slotted Ground Plane

In order to enable future integration of tuning components, specifically varactor diodes, and to improve impedance bandwidth control, two rectangular slots are introduced on the ground plane of the baseline UWB antenna (Antenna 2). These slots are strategically positioned beneath the radiating patch to perturb the surface current distribution and modify the coupling between the patch and ground plane. This modification alters the effective inductance and capacitance of the antenna structure, which in turn influences the resonant modes and helps improve impedance matching across a broader frequency range.

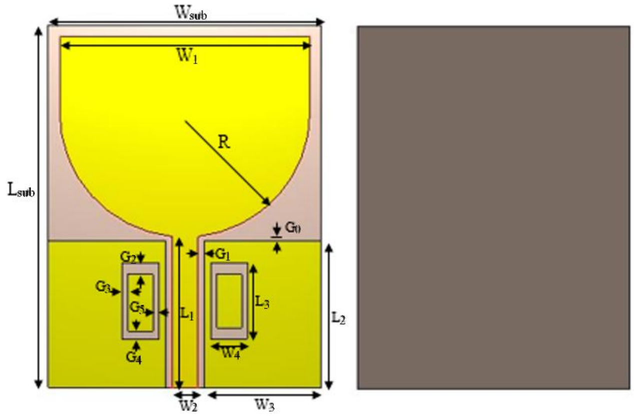

(a) **(b)**

Figure 3. Dimensions of Antenna 2 – Enhanced UWB Antenna with Slotted Ground Plane

Table 2. Dimensions (in mm) of Antenna 2

Parameters	Dimensions (mm)	Parameters	Dimensions (mm)
L_{sub}	32	W_4	3.2
W_{sub}	24	R	11
L_1	13.36	G_0	0.3
L_2	13	G_1	0.55
L_3	6.7	G_2	1
W_1	22	G_3	0.5
W_2	2.3	G_4	0.7
W_3	10.3	G_5	0.5

In addition to enhancing ultra-wideband performance, the inclusion of these ground-plane slots serves a dual purpose: they provide physical space and electromagnetic isolation points for varactor diode placement in subsequent design stages. The improved current distribution introduced by the slots ensures a more controlled tuning mechanism when the varactors are added. **Figure 3** illustrates the layout and physical dimensions of the modified UWB antenna with ground-plane slots, while **Table 2** summarizes the key geometrical parameters. This intermediate design represents a critical step in the antenna evolution, bridging the baseline UWB structure and the tunable configuration developed later.

2.2 Antenna 3 – Reconfigurable UWB-to-Narrowband Antenna using Varactor Diodes

The third configuration, Antenna 3 – Reconfigurable UWB-to-Narrowband Antenna Using Varactor Diodes, introduces active bandwidth tunability to the enhanced UWB design by integrating two SMV1405-040LF varactor diodes. This design enables voltage-controlled reconfiguration of the antenna's operational bandwidth, allowing a transition from ultra-wideband (UWB) performance to a confined narrowband response. The objective of this stage is to validate a dynamic tuning mechanism suitable for adaptive metasurfaces in IRS-enabled 6G systems. **Figure 4** illustrates the layout and key dimensions of the reconfigurable antenna. Antennas 3 and 4 inherit their geometry and physical dimensions from Antenna 2 – the Enhanced UWB Antenna with Slotted Ground Plane – which demonstrated stable broadband behavior. This structural consistency ensures that observed performance variations between configurations are solely due to the presence or absence of the tuning components, enabling a controlled evaluation of practical reconfigurability versus ideal switching.

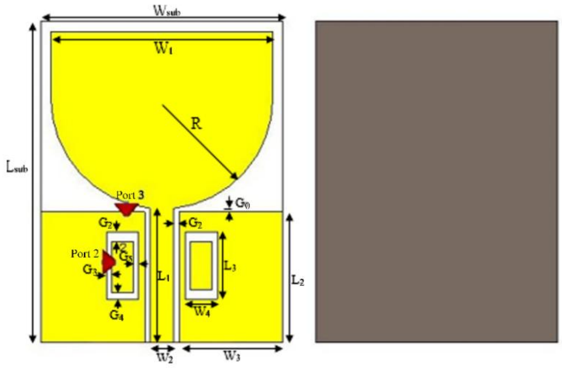

(a) **(b)**

Figure 4. Dimensions of Antenna 3 – Reconfigurable UWB-to-Narrowband Antenna using Varactor Diodes: (a) Top view; (b) Bottom view

The two varactor diodes are strategically placed based on current distribution analysis to maximize bandwidth modulation and frequency agility. The first diode, positioned at Port 2, bridges the ground-plane slot to the adjacent ground region, enabling capacitive control of the ground current path and tuning of the input impedance. The second diode, connected at Port 3, links the main radiating patch to the extended ground, introducing a reactive load that modifies the resonance behavior. These placements are optimized to ensure effective tuning without significantly degrading radiation efficiency. Tuning is achieved by reverse-biasing the diodes at different voltage levels. At 0 V, the Port 2 varactor provides 2.67 pF capacitance, while Port 3 is biased at 1 V, yielding 1.84 pF. For practical implementation, the DC biasing network is designed using high-impedance microstrip lines connected to the diode terminals, isolated from the primary RF signal pathways via chip inductors acting as RF chokes (RFC). This network ensures minimal leakage of the RF signal into the power supply. While the current evaluation focuses on the critical transition to the 5.5 GHz WLAN band, varying the capacitance continuously from 0.5 pF to 5.0 pF provides a agile multi-state response, shifting the narrowband resonance dynamically across a wider tuning spectrum. These values, selected through parametric analysis, confine the operating band to a WLAN-relevant range of 5.11–5.83 GHz. This configuration confirms the feasibility of voltage-controlled UWB-to-narrowband switching using compact varactor integration which is a critical feature for future IRS unit cells requiring on-demand spectral selectivity in 6G communication environments.

2.3 Antenna 4 – Reference Model with Copper Bridges for Ideal Switching Simulation

In order to validate the tuning performance of Antenna 3 – Reconfigurable UWB-to-Narrowband Antenna Using Varactor Diodes, a reference configuration, Antenna 4 – Ideal Switch Reference Model, is developed by replacing each varactor diode with a copper bridge. This configuration, illustrated in

Figure 5, approximates an ideal switching condition, enabling direct comparison between reconfigurable (active) and static (passive) states without the nonlinearities or biasing complexities associated with real semiconductor components. Each copper bridge acts as a highly conductive, linear interconnection, introducing negligible parasitic capacitance or inductance. It effectively emulates a short-circuit condition across the diode terminals, representing the limit case of maximum capacitance (or zero impedance). A 1.5 × 0.4 mm² rectangular copper strip is used to replace each SMV1405-040LF varactor diode at the same physical locations (Ports 2 and 3).

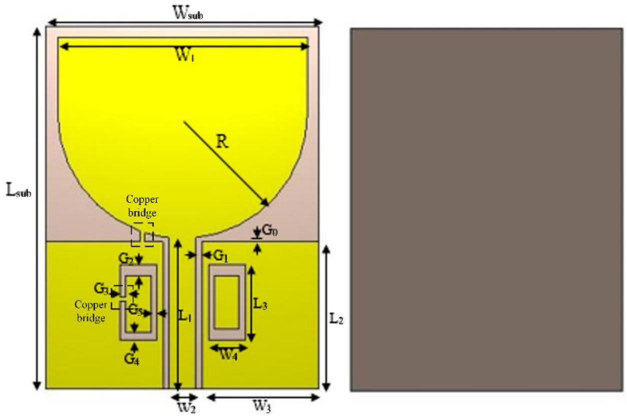

(a) **(b)**

Figure 5. Dimensions of Antenna 4 – Reference Model with Copper Bridges for Ideal Switching Simulation: (a) Top view; (b) Bottom view

These dimensions are matched to the original diode footprint to preserve the local electromagnetic environment and ensure that any performance differences arise solely from the switching element properties. This reference model provides a controlled basis for evaluating the practical impact of varactor diode integration on antenna behavior. By comparing S-parameters and radiation characteristics between Antennas 3 and 4, the influence of the varactor's intrinsic capacitance, series resistance, and voltage-dependent nonlinearity can be isolated. This comparison is critical for validating simulation models and understanding the limitations of real-world tuning mechanisms in reconfigurable antenna designs intended for IRS-based 6G applications.

3. RESULTS AND ANALYSIS

This section presents and discusses the simulation results obtained using CST Microwave Studio®. The analysis is organized into four key performance metrics: reflection coefficient, radiation patterns, gain and efficiency, and surface current distribution. These results are evaluated for all four antenna configurations (Antenna 1, 2, 3, and 4) to assess the impact of structural and functional modifications on electromagnetic behavior.

3.1 Reflection Coefficient

The reflection coefficient ($|S_{11}|$) provides critical insight into impedance matching and frequency selectivity, both of which are essential for effective wave manipulation in IRS-based metasurfaces. **Figure 6** illustrates the $|S_{11}|$ profiles of the four antenna configurations: Antenna 1 – Baseline UWB

Antenna, Antenna 2 – Improved UWB Antenna with Ground-Plane Slots, Antenna 3 – Reconfigurable UWB-to-Narrowband Antenna using Varactor Diodes, and Antenna 4 – Ideal Switch Reference Model.

Antenna 1 achieves a wide impedance bandwidth spanning from 3.22 GHz to 11.26 GHz, with a reflection coefficient consistently below –10 dB, validating its classification as an ultra-wideband (UWB) antenna. The addition of ground-plane slots in Antenna 2 preserves a comparable bandwidth (3.24–11.21 GHz), while improving design flexibility for subsequent tuning stages. This enhancement makes Antenna 2 a suitable base for reconfigurable architectures. In Antenna 3, the integration of SMV1405-040LF varactor diodes introduces voltage-controlled tunability, enabling the antenna to transition from UWB to a narrowband profile. When biased appropriately, Antenna 3 exhibits a sharp resonance with a reflection coefficient dip of –19.65 dB centered at 5.56 GHz, and a reduced bandwidth from 5.11 GHz to 5.83 GHz. This selective tuning aligns well with the WLAN frequency band, showcasing the antenna's capability for adaptive bandwidth control, a key requirement for intelligent beam shaping in IRS-enabled 6G systems. In order to validate the effectiveness of this tuning mechanism, Antenna 4 replaces the varactor diodes with copper bridges, simulating an ideal short-circuit condition. The resulting response shows a narrowband profile from 5.17 GHz to 6.05 GHz, with a reflection coefficient of –19.60 dB at 5.82 GHz. The slight frequency shift relative to Antenna 3 is attributed to the elimination of parasitic capacitance and series resistance associated with real varactors.

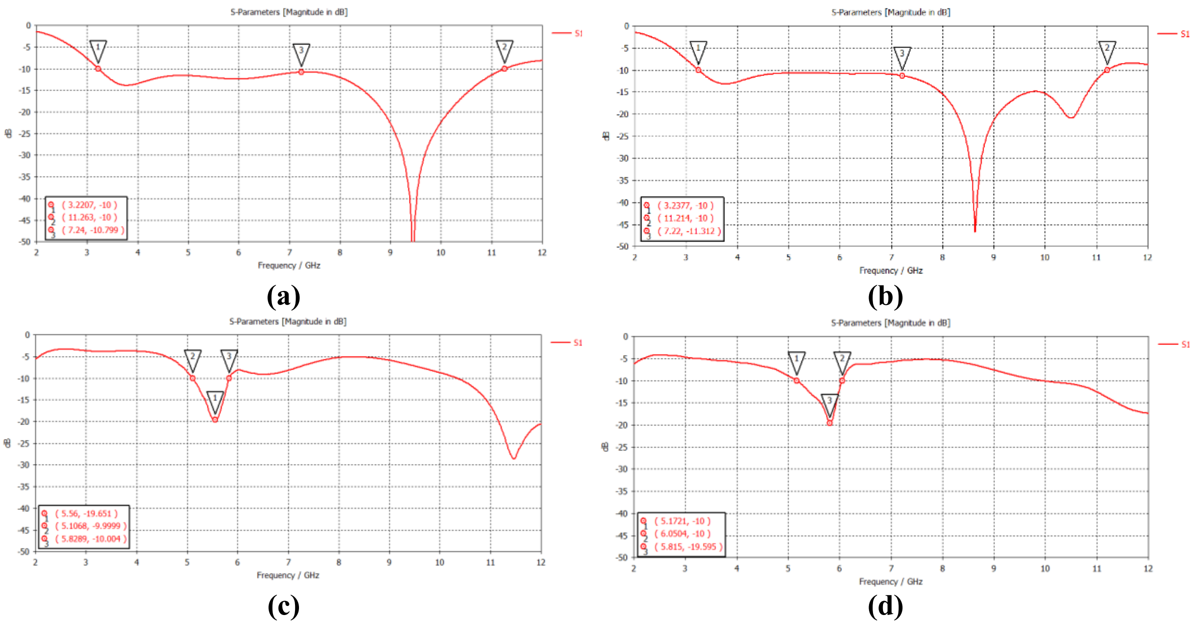

Figure 6. Reflection coefficients for four different antenna configurations: (a) Antenna 1; (b) Antenna 2; (c) Antenna 3; (d) Antenna 4

This progressive shift from a UWB response (Antennas 1 and 2) to a reconfigurable narrowband response (Antennas 3 and 4) demonstrates practical bandwidth control and validates the use of voltage-tunable elements for reconfigurable antenna systems. Such capabilities are pivotal for optimizing spectral utilization and enhancing signal directionality in Ka-band IRS deployments for next-generation 6G networks.

3.2 Radiation Patterns

Directional control of radiation is a critical requirement for intelligent reflecting surface (IRS) metasurfaces, where each unit element must precisely reflect or redirect incident signals. Radiation characteristics were evaluated in both the E-plane and H-plane across key frequencies to assess each antenna's beam behavior.

For Antenna 1 and Antenna 2, the radiation patterns display bidirectional behavior in the *E*-plane and omnidirectional characteristics in the *H*-plane across the entire UWB range (3.2–11.2 GHz). At higher frequencies, the patterns begin to fragment due to the excitation of higher-order modes, which introduces multiple nulls and side lobes. However, the omnidirectionality in the *H*-plane remains largely preserved. Due to the minimal variation in directional behavior across this broad band, radiation plots for Antennas 1 and 2 are omitted here for clarity and to maintain focus on the tunable designs. Instead, **Figure 7** presents the radiation patterns of Antenna and Antenna 4. These two configurations share identical physical geometry, allowing for a controlled comparison of tuning mechanisms. Antenna 3, when biased for narrowband operation, exhibits a more unidirectional pattern in the *E*-plane and maintains a clean omnidirectional pattern in the *H*-plane at 5.56 GHz which correspond to the frequency where its $|S_{11}|$ reaches a deep minimum. This behavior is consistent with the design objective of selectively enhancing directivity within a targeted frequency range. In Antenna 4, the copper bridges replace the varactor diodes to simulate ideal switching behavior, eliminating the effects of parasitic resistance and nonlinearity. The radiation pattern at 5.82 GHz at the point of maximum reflection coefficient for this configuration shows slightly improved main lobe gain compared to Antenna 3 (2.71 dBi vs. 1.96 dBi), with similar directional features in both planes. This slight gain enhancement reflects the reduced insertion loss under ideal switching conditions.

Overall, the results confirm that integrating tunability through varactor diodes does not significantly degrade radiation behavior. On the contrary, it enables dynamic reconfiguration while preserving omnidirectionality in the *H*-plane and improving directionality in the *E*-plane, both of which are advantageous traits for beam steering in Ka-band IRS metasurfaces for future 6G systems.

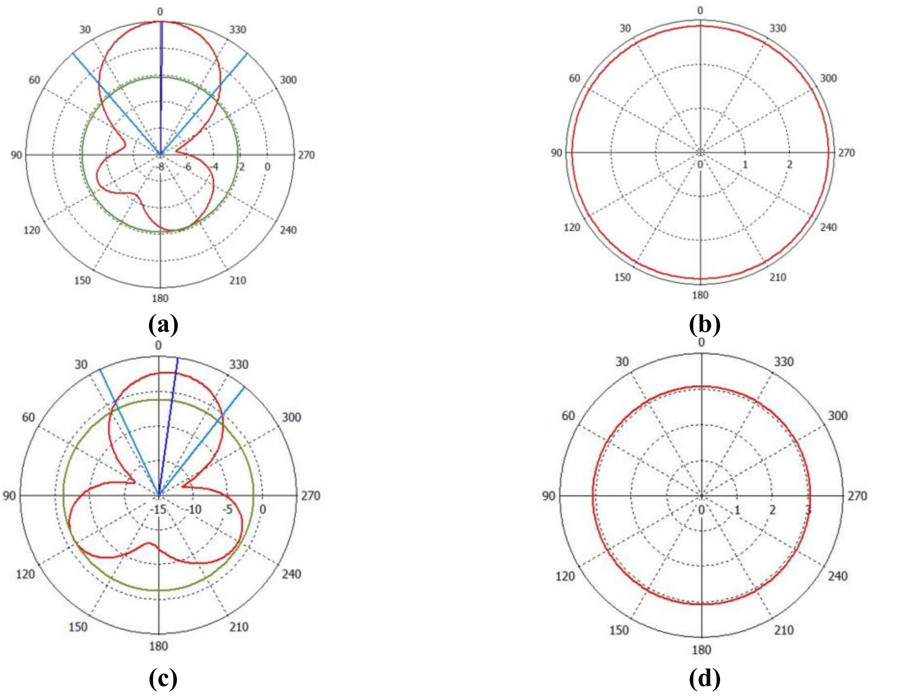

Figure 7. Simulated radiation patterns of the finalized antenna configurations: (a) and (b) Antenna 3 at 5.56 GHz; (c) and (d) Antenna 4 at 5.82 GHz. Subfigures (a) and (c) present the E-plane co-polarization patterns, while (b) and (d) show the H-plane co-polarization patterns

3.3 Gain and Radiation Efficiency

The gain and radiation efficiency of all four antenna configurations were analyzed to evaluate their viability for integration into intelligent reflecting surface (IRS) metasurfaces. In order to properly benchmark the performance of the proposed design against existing implementations, **Table 3** compares this work with previously reported reconfigurable antenna architectures.

Antenna 1 exhibited robust broadband performance, with gain increasing from 2.43 dBi at 3.22 GHz to 5.20 dBi at 11.26 GHz, and radiation efficiency ranging from 85.74% to 79.32% across the band. These results validate its effectiveness as a foundational design for subsequent reconfigurable stages. Antenna 2 preserved similar broadband characteristics, with gain values of 2.44 dBi at 3.24 GHz and 5.33 dBi at 11.21 GHz, and slightly reduced efficiency of 77.10% at the upper frequency. The minor loss introduced by the ground-plane slots confirms the design's compatibility with further tuning mechanisms. Antenna 3 achieved a gain of 3.56 dBi and radiation efficiency of 73.89% at the tuned center frequency of 5.56 GHz. The slight reduction in efficiency compared to the broadband designs is attributed to parasitic resistance and capacitive losses introduced by the varactor diodes. Nonetheless, the design demonstrates acceptable trade-offs for dynamic tuning, making it suitable for adaptive IRS unit cells where flexibility often outweighs minor efficiency penalties. Antenna 4 attained a higher gain of 4.27 dBi and efficiency of 71.41% at 5.82 GHz, corresponding to its optimal narrowband response. The gain improvement, despite a marginal drop in efficiency, reinforces the conclusion that the core antenna structure is electromagnetically robust, and that performance degradation in Antenna 3 is primarily due to the real-world limitations of the tuning components.

Table 3. Comparison with previous reconfigurable antenna studies

Reference	Substrate	Tuning element	Reconfiguration Type	Operating Frequency (GHz)	Peak Gain (dBi)	Efficiency (%)
[10]	RO4003	Varactor	Frequency / Pattern	1.70 – 2.20	9.00	61.3 – 90.8
[14]	R-5785N / R-5680N	Varactor	Frequency Dual-Pol	23.20 – 30.20	8.90– 10.50	60.0 – 70.0
[18]	Rogers RT5880	PIN + Varactor	Frequency / Bandwidth	3.19–5.56 (WB) / 3.40–5.32 (NB)	6.02 / 5.37	57.0 – 97.0
This work	FR-4	Varactor	UWB-to-Narrowband	3.22 – 11.26 to 5.11 – 5.83	3.56 (Narrow)	73.89

In order to maintain visual clarity and highlight the designs most relevant to IRS applications, **Figure 8** presents the gain and efficiency results for Antenna 3 and Antenna 4 only. While Antennas 1 and 2 establish the design evolution, their broadband characteristics and lack of reconfigurability render them secondary in the context of tunable IRS metasurfaces.

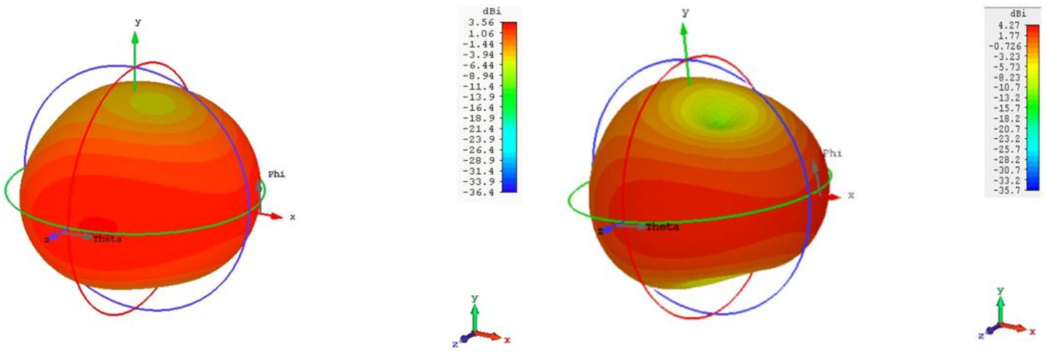

(a) **(b)**

Figure 8. Simulated 3D realized gain distributions of the finalized antenna configurations: (a) Antenna 3 at 5.56 GHz; (b) Antenna 4 at 5.82 GHz. Each frequency corresponds to the minimum reflection coefficient of the respective design. [Note: Accompanying numerical radiation efficiencies are recorded textually as 73.89% and 71.41% respectively]

3.4 Surface Current Distribution

Surface current distribution analysis offers critical insight into the electromagnetic behavior of the antenna, particularly in understanding how tuning components influence resonance characteristics and radiation performance.

In the baseline UWB design (Antenna 1) and the enhanced version with ground-plane slots (Antenna 2), surface currents are predominantly concentrated along the feed line and the edges of the radiating patch, with minimal involvement from the ground plane. In Antenna 2, additional current density appears near the edges of the ground-plane slots, confirming their role in modifying impedance and enhancing tuning sensitivity. By contrast, the tunable design with varactor diodes (Antenna 3) exhibits significantly altered current pathways. High current concentrations are observed around the locations of the two varactor diodes, indicating that these components actively perturb the local electromagnetic field and contribute to frequency reconfigurability. The reactive loading introduced by the varactors enables controlled modification of the antenna's resonant behavior via bias-dependent capacitance. In the reference model with copper bridges (Antenna 4), the current follows similar paths to those seen in Antenna 3 but with smoother, more continuous flow across the bridge areas. This reflects the effect of ideal low-loss switching and validates the tuning locations selected for the varactor integration. The absence of parasitic losses in the copper-bridged configuration highlights the intrinsic tuning potential of the geometry itself, independent of component nonidealities.

In order to maintain visual focus, **Figure 9** presents the surface current distributions for Antennas 3 and 4 only. These represent the finalized and tunable antenna designs, which are most relevant for intelligent metasurface applications. Antennas 1 and 2 are excluded from the figure due to their standard, broadband current behavior, which primarily serves as a reference for evaluating the impact of reconfigurable elements.

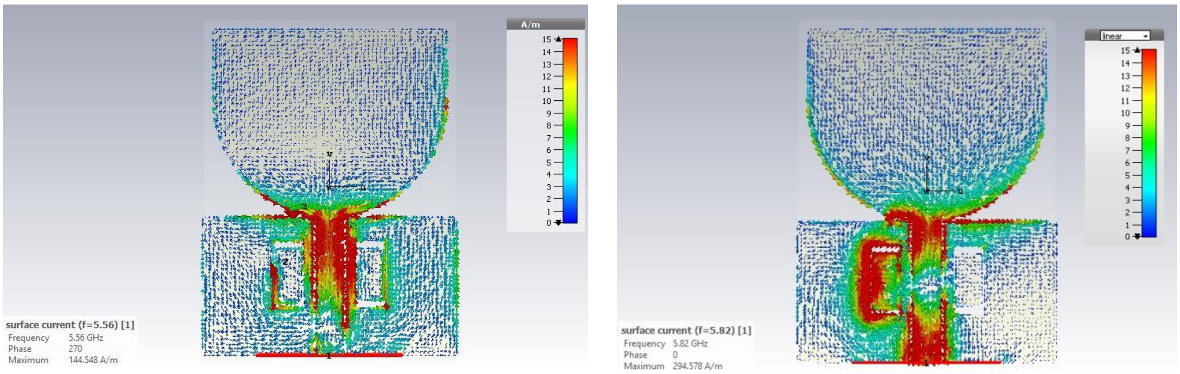

(a) **(b)**

Figure 9. Surface current distributions of the finalized antenna configurations: (a) Antenna 3 at 5.56 GHz; (b) Antenna 4 at 5.82 GHz

4. CONCLUSION

This work presented the design and evaluation of a UWB-to-narrowband reconfigurable antenna using varactor diodes, targeting intelligent reflecting surface (IRS) applications in the Ka-band for future 6G wireless systems. The reconfigurable mechanism validated at 5 GHz serves as a foundation, and with dimensional scaling and material substitution, the same architecture can be effectively deployed in Ka-band IRS systems. The study progressed from a baseline ultra-wideband (UWB) antenna through successive structural enhancements, including ground-plane slotting and varactor integration, resulting in two finalized configurations: Antenna 3 (varactor-loaded) and Antenna 4 (copper-bridged reference). Both designs share identical geometries, enabling a direct comparison between practical and ideal tuning conditions. Reflection coefficient analysis demonstrated that the varactor-loaded antenna effectively reconfigures its impedance bandwidth, achieving a narrowband response centered at 5.56 GHz with a reflection coefficient of –9.65 dB which is well aligned with the WLAN band. The reference model using copper bridges exhibited similar behavior at 5.82 GHz with a peak reflection coefficient of –19.60 dB, validating the tunability of the design under ideal low-loss conditions. Radiation pattern results showed that both tunable and reference antennas maintain a consistent H-plane omnidirectionality and exhibit improved E-plane directionality near their respective resonant frequencies. This demonstrates that the introduction of varactor diodes does not degrade core radiation characteristics and supports the beamforming requirements of IRS metasurfaces. The gain and efficiency analysis further confirmed the practical feasibility of the tunable design. Antenna 3 achieved a gain of 3.56 dBi and radiation efficiency of 73.89% at 5.56 GHz, while Antenna 4 reached 4.27 dBi and 71.41% efficiency at 5.82 GHz. These results highlight that the performance penalties from varactor-induced parasitics remain within acceptable bounds for dynamically tunable IRS applications. Surface current distribution analysis reinforced the role of the varactors in reshaping current flow at critical locations, enabling effective frequency control without compromising the antenna's radiative behavior. In summary, the proposed reconfigurable antenna demonstrates a reliable transition from UWB to narrowband operation through voltage-controlled tuning. Its performance affirms the suitability of varactor-based approaches for enabling dynamic resonance control in compact IRS unit cells. These findings provide a practical foundation for scalable, frequency-agile metasurfaces in 6G Ka-band wireless environments. Although fabrication was not carried out within this work due to time and resource limitations, the design of Antenna 3 has been structured with practical implementation in mind. Future work will include prototype fabrication and experimental validation to further substantiate the simulation results presented here.

5. ACKNOWLEDGEMENT

This research was supported by Universiti Tun Hussein Onn Malaysia (UTHM) through Tier 1 (vot Q981).

6. AI USAGE DECLARATION

The authors declare that no generative AI tools were used in the conceptualization, analysis, or interpretation of this work. The AI-assisted tool, Gemini, was used solely for linguistic improvements including grammar and spelling checks. All AI-generated text was carefully reviewed, edited, and verified by the authors to ensure accuracy, academic integrity and originality.

7. REFERENCES

[1] Gupta A, Jha RK. A survey of 5G network: Architecture and emerging technologies. IEEE Access. 2015; 3:1206–1232. https://doi.org/10.1109/access.2015.2461602

[2] Giordani M, Polese M, Mezzavilla M, Rangan S, Zorzi M. Toward 6G networks: Use cases and technologies. IEEE Commun. Mag. 2020;58(3):55–61. https://doi.org/10.1109/mcom.001.1900411

[3] Wu Q, Zhang R. Towards smart and reconfigurable environment: Intelligent reflecting surface aided wireless network. IEEE Commun. Mag. 2020; 58(1) :106–112. https://doi.org/10.1109/mcom.001.1900107

[4] Liaskos C, Nie S, Tsioliaridou A, Pitsillides A, Ioannidis S, Akyildiz IF. A new wireless communication paradigm through software-controlled metasurfaces. IEEE Commun. Mag. 2018;56(9):162–169. https://doi.org/10.1109/mcom.2018.1700659

[5] Hassouna S, Jamshed MA, Rains J, et al. A survey on reconfigurable intelligent surfaces: Wireless communication perspective. IET Commun. 2023;17(5):497-537. https://doi.org/10.1049/cmu2.12571

[6] Di Renzo M, et al. Smart radio environments empowered by reconfigurable intelligent surfaces: How it works, state of research, and road ahead. IEEE J. Sel. Areas Commun. 2020;38(11):2450–2525. https://doi.org/10.1109/jsac.2020.3007211

[7] Balanis CA. Antenna theory: Analysis and design. 4th ed. Hoboken, NJ, USA: Wiley; 2016.

[8] Chen JY, Row JS. Frequency reconfigurable antenna with conical radiation pattern and wide tuning range. Prog. Electromagn. Res. Lett. 2021;96:147–152. https://doi.org/10.2528/pierl21020602

[9] Erdil E, Topalli K, Unlu M, Civi OA, Akin T. Frequency tunable microstrip patch antenna using RF-MEMS technology. IEEE Trans. Antennas Propag. 2007;55(4):1193–1197. https://doi.org/10.1109/tap.2007.893426

[10] Zhang J, Wang B, Yan S, Li W, Vandenbosch GAE. Metamaterial inspired varactor-tuned antenna with frequency reconfigurability and pattern diversity. Sensors. 2024;24(6):1956. https://doi.org/10.3390/s24061956
[11] Chen CY, Chiu CT, Tang HJ, Huang TH, Itoh T. Ka-band beam-scanning leaky-wave antenna fed by reconfigurable spoof surface plasmon polaritons. Opt. Express. 2023;31(8):12189–12199. https://doi.org/10.1364/oe.487068
[12] Malik BT, Khan S, Koziel S. Design and implementation of multi-band reflectarray metasurface for 5G millimeter-wave coverage enhancement. Sci. Rep. 2024;14(1):15286. https://doi.org/10.1038/s41598-024-66330-4
[13] Luo H, Yang X. Frequency-reconfigurable antenna based on epsilon-negative transmission lines. Electron. Lett. 2023;59(3):104–106. https://doi.org/10.1049/ell2.12841
[14] Chen Q, et al. Varactor-based frequency-reconfigurable dual-polarized mm-wave antenna array for mobile devices. IEEE Trans. Antennas Propag. 2023;71(8):6628–6638. https://doi.org/10.1109/tap.2023.3287679
[15] Da Silva LG, Chu Z, Xiao P, A C S Jr. A varactor-based 1024-element RIS design for mm-waves. Front. Commun. Netw. 2023;4:1086011. https://doi.org/10.3389/frcmn.2023.1086011
[16] Rains J, et al. Fully-addressable varactor-based reflecting metasurface with dual-linear polarisation for low power RIS. In: Proc. 17th Eur. Conf. Antennas Propag. (EuCAP); 2023 Mar; Florence, Italy. https://doi.org/10.23919/eucap57121.2023.10133408
[17] Navarajan J, Jebarani MRE, Krishnan VG. Frequency reconfigurable microstrip patch antenna for multiband applications with RF MEMS shunt capacitor switch. Int. J. Intell. Syst. Appl. Eng. 2023;11(3s):1–7. https://doi.org/10.17762/ijritcc.v10i12.5893
[18] Nguyen TK, et al. Frequency-reconfigurable antenna with wide- and narrowband modes for sub-6 GHz cognitive radio. IEEE Antennas Wirel. Propag. Lett. 2023;22(1):64–68. https://doi.org/10.1109/LAWP.2022.3201969

AUTHORS' PROFILES

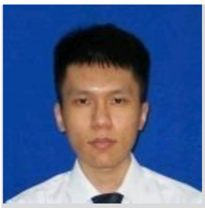

__Chai Han Ming__ received his Bachelor's degree in Electrical Engineering from Universiti Tun Hussein Onn Malaysia (UTHM). Under the supervision of Assoc. Prof. Dr. Shaharil bin Mohd Shah, his research focused on reconfigurable RF systems. His Final Year Project, "UWB to Narrowband Tunable Antenna with Varactor Diodes," involved designing frequency-agile antennas capable of switching between Ultra-Wideband and specific narrowband frequencies. His research interests include microwave engineering, tunable RF components, and wireless communication technologies.

Assoc. Prof. __Dr. Shaharil Mohd Shah__ (Member, IEEE) is with the Department of Communication Engineering at Universiti Tun Hussein Onn Malaysia (UTHM). He received his B.Eng. from Multimedia University (MMU) (2002), M.Sc. from the University of Surrey, U.K. (2004), and Ph.D. from the University of Birmingham, U.K. (2016). His research expertise encompasses the design of microwave devices, reconfigurable antennas, active antenna measurements, and the nonlinear characterization of active devices. He currently leads academic and research initiatives within the Faculty of Electrical and Electronic Engineering at UTHM.

Assoc. Prof. __Dr. Huda A. Majid__ is the Head of Program for Bachelor of Electronic Engineering Technology at Universiti Tun Hussein Onn Malaysia (UTHM). He earned his Ph.D. in Electrical Engineering from Universiti Teknologi Malaysia (UTM), followed by a post-doctoral fellowship. With a Scopus H-index of 21, he has authored over 100 international publications and secured grants exceeding RM200k. His research expertise includes planar and flexible antennas, reconfigurable arrays, metamaterials, RF/microwave devices, and IoT applications. Dr. Huda currently leads academic and research initiatives within the Department of Electrical Engineering Technology at UTHM's Pagoh Campus.

Assoc. Prof. ***Dr. Zuhairiah Zainal Abidin*** *is an Associate Professor in the Department of Electronic Engineering at Universiti Tun Hussein Onn Malaysia (UTHM). She earned her B.Eng. from Universiti Teknologi Malaysia (UTM) and her Ph.D. from the University of Bradford, U.K.. Her research focuses on MIMO antennas, wearable antennas, metamaterial resonators, and electromagnetic bandgap (EBG) applications for wireless systems and sensors. She has extensive publications in RF and microwave engineering.*

Dr. Saizal Md Mustam *is a Senior Lecturer at Universiti Tun Hussein Onn Malaysia (UTHM) and currently serves as the Deputy Director of Research Grant Management at the Research Management Centre. He earned his B.Eng. and M.Eng. from UTHM and his Ph.D. from Universiti Teknologi Malaysia (UTM). His research expertise includes electromagnetic compatibility (EMC), diffusion-based molecular communication, and RF/microwave devices. As a Principal Researcher at the Faculty of Electrical and Electronic Engineering, he actively contributes to advancing wireless communication technologies and electromagnetic research, supporting UTHM's academic and research management initiatives.*

Assoc. Prof. ***Dr. Nor Surayahani Suriani*** *is an Associate Professor at Universiti Tun Hussein Onn Malaysia (UTHM). She obtained her B.Eng. from Universiti Putra Malaysia (UPM), M.Eng. from Universiti Teknologi Malaysia (UTM), and Ph.D. from Universiti Kebangsaan Malaysia (UKM). Her expertise lies in image processing and computer vision, with research focusing on healthcare and safety applications. Her work includes sudden fall classification and bio-signal extraction using deep learning techniques. She has authored numerous international publications and leads research projects in electrical and electronic engineering, emphasizing automated monitoring, intelligent systems, and advanced signal.*

Munirah Az Zahra Abdul Rashid *received her Master's degree in Electrical Engineering (by research mode) from the Faculty of Electrical and Electronic Engineering (FKEE) at Universiti Tun Hussein Onn Malaysia (UTHM). Her postg raduate research, conducted with the Advanced Telecommunication Research Center (ATRC), focused on compact triple-notch band ultra-wideband (UWB) antennas and interference mitigation. Currently, she is an R&D Applications professional at Avery Dennison Smartrac in Kulim, Kedah. Her expertise and research interests include RFID technology, RF and microwave engineering, and the development of innovative wireless communication systems for industrial applications.*